Interconversion and Reactivity of Two Heterometallic Tin-Containing Cuboidal Clusters from $[Mo_3S_4(H_2O)_9]^{4+}$: X-ray Structure of the Single Cube with an Mo_3SnS_4 Core

Jane E. Varey, Gert J. Lamprecht, Vladimir P. Fedin, Alvin Holder, William Clegg, Mark R. J. Elsegood, and A. Geoffrey Sykes*

Department of Chemistry, University of Newcastle, Newcastle upon Tyne NE1 7RU, U.K.

Received December 28, 1995[⊗]

The $Mo_3SnS_4^{6+}$ single cube is obtained by direct addition of Sn^{2+} to $[Mo_3S_4(H_2O)_9]^{4+}$. UV−vis spectra of the product (0.13 mM) in 2.00 M $HClO_4$, Hpts, and HCl indicate a marked affinity of the Sn for Cl^-, with formation of the more strongly yellow $[Mo_3(SnCl_3)S_4(H_2O)_9]^{3+}$ complex complete in as little as 0.050 M Cl^-. The X-ray crystal structure of $(Me_2NH_2)_6[Mo_3(SnCl_3)S_4(NCS)_9]\cdot 0.5H_2O$ has been determined and gives Mo−Mo (mean 2.730 Å) and Mo−Sn (mean 3.732 Å) distances, with a difference close to 1 Å. The red-purple double cube cation $[Mo_6SnS_8(H_2O)_{18}]^{8+}$ is obtained by reacting Sn metal with $[Mo_3S_4(H_2O)_9]^{4+}$. The double cube is also obtained in ∼50% yield by BH_4^- reduction of a 1:1 mixture of $[Mo_3SnS_4(H_2O)_{10}]^{6+}$ and $[Mo_3S_4(H_2O)_9]^{4+}$. Conversely two-electron oxidation of $[Mo_6SnS_8(H_2O)_{18}]^{8+}$ with $[Co(dipic)_2]^-$ or $[Fe(H_2O_6]^{3+}$ gives the single cube $[Mo_3SnS_4(H_2O)_{12}]^{6+}$ and $[Mo_3S_4(H_2O)_9]^{4+}$ (up to 70% yield), followed by further two-electron oxidation to $[Mo_3S_4(H_2O)_9]^{4+}$ and Sn^{IV}. The kinetics of the first stages have been studied using the stopped-flow method and give rate laws first order in $[Mo_6SnS_8(H_2O)_{18}]^{8+}$ and the Co^{III} or Fe^{III} oxidant. The oxidation with $[Co(dipic)_2]^-$ has no $[H^+]$ dependence, $[H^+] = 0.50-2.00$ M. With Fe^{III} as oxidant, reaction steps involving $[Fe(H_2O)_6]^{3+}$ and $[Fe(H_2O)_5OH]^{2+}$ are implicated. At 25 °C and $I = 2.00$ M (Li(pts)) k_{Co} is 14.9 M^{-1} s^{-1} and k_a for the reaction of $[Fe(H_2O)_6]^{3+}$ is 0.68 M^{-1} s^{-1} (both outer-sphere reactions). Reaction of Cu^{2+} with the double but not the single cube is observed, yielding $[Mo_3CuS_4(H_2O)_{10}]^{5+}$. A redox-controlled mechanism involving intermediate formation of Cu^+ and $[Mo_3S_4(H_2O)_9]^{4+}$ accounts for the changes observed.

Introduction

A number of heterometal-containing cuboidal clusters have been prepared from the trinuclear cuboidal (metal depleted) Mo^{IV}_3 complex $[Mo_3S_4(H_2O)_9]^{4+}$.[1,2] Three structure types have been identified in crystallographic studies, the single clusters **I** (e.g. M = Fe, Ni, Pd, In),[3−6] corner-shared (or sandwich[1]) clusters **II** (M = Hg, Sn, Sb),[7,9,10] and edge-linked clusters **III** (M = Co, Cu, Pd).[5,7,8,11] Solution kinetic and thermodynamic properties have been studied in the case of the Fe-,[12] Ni-,[13] and Cu-containing[14] clusters. The clusters with heterometallic atoms Sn[9] (and In[6]) are unusual in giving both single and double cube structures **I** and **II**, whereas Co,[7,8] Cu,[11] and Pd[5] give structures **I** and **III**. In this and a subsequent paper,[15] we study the interrelationship of such forms with Sn (present paper) and Pd as chosen examples. The structures proposed for the single and double cubes are as illustrated:[9]

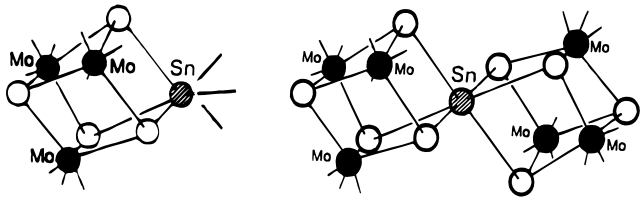

$[Mo_3SnS_4(H_2O)_{12}]^{6+}$ $[Mo_6SnS_8(H_2O)_{18}]^{8+}$

The two clusters are yellow-green and red-purple, respectively. The first X-ray characterization of the single $Mo_3SnS_4^{6+}$ cluster is included in this paper, alongside kinetic and thermodynamic studies on the aqueous solution chemistry of both cuboidal clusters.

Experimental Section

Preparation of $[Mo_3S_4(H_2O)_9]^{4+}$. The procedure used was the BH_4^- reduction of the dinuclear cysteinato Mo^{V}_2 complex $Na_2[Mo_2O_2(\mu\text{-}S)_2(cys)_2]\cdot 4H_2O$ to give the cuboidal complex $[Mo_4S_4(H_2O)_{12}]^{5+}$.[16] On heating of the latter for 3−4 h at ∼90 °C, the green trinuclear Mo^{IV}_3 product $[Mo_3S_4(H_2O)_9]^{4+}$ was obtained quantitatively and was purified by Dowex 50W-X2 cation-exchange chromatography. Stock solutions (∼5 mM) in 2 M *p*-toluenesulfonic acid (Hpts) gave UV−vis

[⊗] Abstract published in *Advance ACS Abstracts,* August 1, 1996.

(1) Shibahara, T. *Adv. Inorg. Chem.* **1991**, *37*, 143−173; *Coord. Chem. Rev.* **1993**, *123*, 73−147.
(2) Saysell, D. M.; Sykes, A. G. *J. Clust. Sci*. **1995**, *6*, 449.
(3) Shibahara, T.; Akashi, H.; Kuroya, H. *J. Am. Chem. Soc.* **1986**, *108*, 1342.
(4) Shibahara, T.; Yamasaki, M.; Akashi, H.; Katayama, T. *Inorg. Chem.* **1991**, *30*, 2693.
(5) Murata, T.; Mizobe, Y.; Gao, H.; Ishii, Y.; Wakabayashi, T.; Nakano, F.; Tanase, T.; Yano, S.; Hidai, M.; Echizen, I.; Namikawa, H.; Motomura, S. *J. Am. Chem. Soc.* **1994**, *116*, 3389.
(6) (a) Sakane, G.; Shibahara, T. *Inorg. Chem.* **1993**, *32*, 777. (b) Sakane, G.; Yao, Y.-G.; Shibahara, T. *Inorg. Chim. Acta* **1994**, *216*, 13.
(7) Shibahara, T.; Akashi, H.; Yamasaki, M.; Hashimoto, K. *Chem. Lett.* **1991**, 689.
(8) Shibahara T.; Akashi, H.; Hashimoto, K. *J. Inorg. Biochem.* **1989**, *36*, 178.
(9) Shibahara, T.; Akashi, H. *Inorg. Chem.* **1989**, *28*, 2906.
(10) Shibahara, T.; Hashimoto, K.; Sakane, G. *J. Inorg. Biochem.* **1991**, *43*, Abstract D047.
(11) Akashi, H.; Kuroya, H.; Shibahara, T. *J. Am. Chem. Soc.* **1988**, *110*, 3314.
(12) Dimmock, P. W.; Dickson, D. P. E.; Sykes, A. G. *Inorg. Chem.* **1990**, *29*, 5120.
(13) (a) Dimmock, P. W.; Lamprecht, G. J.; Sykes, A. G. *J. Chem. Soc., Dalton Trans.* **1991**, 955. (b) Saysell, D. M.; Borman, C. D.; Kwak, C.-H.; Sykes, A. G. *Inorg. Chem.* **1996**, *35*, 173.
(14) Nasreldin, M.; Li, Y.-J.; Mabbs, M. E.; Sykes, A. G. *Inorg. Chem.* **1994**, *33*, 4283.
(15) Saysell, D. M.; Lamprecht, G. J.; Darkwa, G. J.; Sykes, A. G. *Inorg. Chem.* **1996**, *35*, 5531.
(16) Martinez, M.; Ooi, B.-L.; Sykes, A. G. *J. Am. Chem. Soc.* **1987**, *109*, 4615.

S0020-1669(95)01659-4 CCC: $12.00

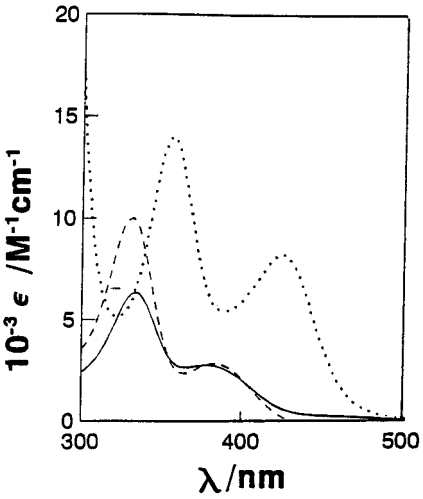

Figure 1. UV−vis spectra of $Mo_3SnS_4^{6+}$ (ϵ's per Mo_3) in 2.0 M acids: Hpts (—); $HClO_4$ (- - -); HCl (•••).

absorbance peaks λ/nm (ϵ/M^{-1} cm^{-1} per Mo_3) at 366 (5550) and 603 (362).[17] Overall yields were 10−20%.

Preparation of Aquatin(II) Solutions.[18] Tin shot (Aldrich; ∼3 mm diameter) was washed with 2 M HCl, H_2O, and then 0.5 M Hpts. The metal was dried with absorbant paper and put into a 25 mL conical flask under N_2. A solution of copper(II) (∼0.05 M) was prepared by loading copper(II) perchlorate onto a Dowex 50W-X2 column and eluting with 0.50 M Hpts or $HClO_4$. Standardization was carried out by measuring the absorbance at the 803 nm peak (ϵ = 11.9 M^{-1} cm^{-1} determined for $CuSO_4$). The Cu^{II} solution was added to excess Sn metal, and the N_2 bubbling was continued. The flask was covered with Al foil to avoid possible effects of light. The reactant solution became colorless and was left for a further 1 h to ensure complete conversion to Sn^{II}. The tin solution was then filtered to remove the copper produced and any remaining tin metal. The Sn^{II} concentration was calculated from the amount of Cu^{II} used by assuming quantitative conversion, (1).

$$Sn + Cu^{II} \rightarrow Sn^{II} + Cu \quad (1)$$

Solutions of Sn^{II} in Hpts in air gave a white precipitate on standing overnight that became yellow over several days. Solutions of ∼50 mM $SnCl_4 \cdot 5H_2O$ (BDH) in 1 M acid (HCl, Hpts, or $HClO_4$) gave no precipitate on standing over extended periods (weeks).[19]

Preparation of $[Mo_3SnS_4(H_2O)_{12}]^{6+}$. A 2-fold excess of Sn^{II} in 0.5 M Hpts was added air-free to $[Mo_3S_4(H_2O)_9]^{4+}$ (∼5 mM) in 2.0 M Hpts. An immediate change to green-yellow was observed, (2). The

$$Mo_3S_4^{4+} + Sn^{2+} \rightarrow Mo_3SnS_4^{6+} \quad (2)$$

product in 0.5 M Hpts was loaded onto a Dowex 50W-X2 column, washed with 0.5, 1.0, and 2.0 M Hpts and the $[Mo_3SnS_4(H_2O)_{12}]^{6+}$ product eluted with 3.0 M Hpts as a yellow-brown band. No green $[Mo_3S_4(H_2O)_9]^{4+}$ band was observed. The procedure was repeated using different acids, and spectra in 2.0 M Hpts, $HClO_4$, and HCl are shown in Figure 1. Peak positions and absorption coefficients are listed in Table 1.

No red-purple color of the double cube, characteristic peaks at 380 and 545 nm, was observed during the column chromatography. With slow bubbling of air through solutions, there is ∼25% decay in 1 h. Column chromatography gives a green product characterized by the UV−vis spectrum as $[Mo_3S_4(H_2O)_9]^{4+}$ and a yellow band at the top of the column believed to be unreacted cube and Sn^{IV} oxo/hydroxo product.

Table 1. Details of UV−Vis−Near-IR Aqueous Solution Absorption Spectra

cluster	acid used	peaks: λ/nm (ϵ/M^{-1} cm^{-1})
$[Mo_3SnS_4(H_2O)_{12}]^{6+}$ [a]	2.0 M Hpts	331 (6330), 375 (2817), 560 (380), 644 (380)
	2.0 M Hpts[c]	560 (345), 644 (327)
	2.0 M $HClO_4$	331 (10 010), 382 (∼2900)
	2.0 M HCl	356 (14 030), 424 (8260)
$[Mo_6SnS_8(H_2O)_{18}]^{8+}$ [b]	2.0 M Hpts	310 (∼10^4), 379 (22 100),[d] 544 (15 500), 930 (400)
	2.0 M Hpts[c]	545 (15 084), 960 (852)

[a] ϵ's per Mo_3. [b] ϵ's per Mo_6. [c] Reference 9; ϵ's quoted per Mo have been converted to values as listed here. [d] Any $[Mo_3S_4(H_2O)_9]^{4+}$ present, peak at 366 nm (ϵ 5550), will contribute to this absorbance. See, e.g.: Varey, J. E. Ph.D. Thesis, University of Newcastle, 1993.

The relevant equation is as in (3). At ∼4 °C and under N_2, the cube

$$2Mo_3SnS_4^{6+} + O_2 + 4H^+ \rightarrow 2Mo_3S_4^{4+} + 2Sn^{IV} + 2H_2O \quad (3)$$

$[Mo_3SnS_4(H_2O)_{12}]^{6+}$ in 2.0 M Hpts is stable over periods of at least 4−6 days.

No reaction is observed on addition of $SnCl_4 \cdot 5H_2O$ (0.2 mL of a 50 mM solution) in 1.0 M HCl and 1.0 M $HClO_4$ to $[Mo_3S_4(H_2O)_9]^{4+}$ (2.5 mL of a 0.35 mM solution) in 2.0 M $HClO_4$.

Preparation of $(Me_2NH_2)_6[Mo_3(SnCl_3)S_4(NCS)_9] \cdot 0.5H_2O$. All procedures were carried out in air. Solid tin(II) chloride, $SnCl_2 \cdot 2H_2O$ (0.20 g), was added to ∼1 mM $[Mo_3S_4(H_2O)_9]^{4+}$ in 2 M HCl (20 mL). The green solution was stirred for 3 min, and sodium thiocyanate, NaNCS (2.0 g), and dimethylammonium chloride, Me_2NH_2Cl (2.0 g), were added. The brown solution was kept at ambient temperature for 3−5 days, when dark brown crystals were filtered off and dried in air. Yield: 0.24g (83%). Anal. Calcd for $C_{21}H_{50}N_{15}Cl_3Mo_3OS_{13}Sn$: C, 17.29; H, 3.46; N, 14.40. Found: C, 17.17; H, 3.60; N, 14.07. The neutral content of solutions was determined by inductively coupled plasma (ICP) atomic emission spectroscopy, which gave Mo:Sn ratios of 3.15:1 and 3.07:1 for different samples in accordance with the above formula. The UV−vis absorption spectrum in acetonitrile gave peak positions λ/nm (ϵ/$M^{-1}cm^{-1}$) at 399 (2.52×10^4) and 754 (1.15×10^3). The IR spectrum in KBr disks gave: ν(CN) 2098 (vs), 1560 (w), 1456 (m), 1402 (m), 1010 (m), ν(CS) 810 (m), and δ(NCS)/ν(MoN)/ν(SnCl) 488 (w), 422 (w), 395 (w) cm^{-1}.

Preparation of $[Mo_6SnS_8(H_2O)_{18}]^{8+}$. Solutions of green $[Mo_3S_4(H_2O)_9]^{4+}$ under N_2 in 2.0 M Hpts were added to tin shot (prepared and washed as described above) in a conical flask also air-free. The color began to change to red-purple almost immediately. In a controlled experiment, no reaction of tin metal with 2.0 M Hpts was observed in ∼1 h (test for Sn^{II} using NaOH[20]). After completion of the reaction (∼1 h), the solution was transferred to a storage vessel. The product (see eq 4) has been characterized previously.[9] The UV−vis spectrum

$$2Mo_3S_4^{4+} + Sn \rightarrow Mo_6SnS_8^{8+} \quad (4)$$

is shown in Figure 2 alongside spectra of $[Mo_3SnS_4(H_2O)_{12}]^{6+}$ and $[Mo_3S_4(H_2O)_9]^{4+}$, all in 2.0 M Hpts. Details of peak positions, Table 1, are in good agreement with previous studies.[9] Solutions could be stored for several days at 4 °C under N_2. On slow bubbling of air through a solution in 2.0 M Hpts at 25 °C, ∼40% decrease in absorbance at 544 nm was observed in 1 h. Scan spectra showed the formation of a peak at ∼330 nm (with a shoulder at 410 nm) and an absorbance decrease at 379 as well as at 544 nm as oxidation of the double cube and the build-up of $[Mo_3SnS_4(H_2O)_{12}]^{6+}$ or related products occur. Column separation of the fully oxidized solutions gave $[Mo_3S_4(H_2O)_9]^{4+}$ and some yellow-orange product, (5). Solutions of $[Mo_6SnS_8(H_2O)_{18}]^{8+}$ could be kept for much longer periods in the presence of Sn metal.

$$2Mo_6SnS_8^{8+} + O_2 + 4H^+ \rightarrow 4Mo_3S_4^{4+} + 2H_2O + 2Sn^{IV} \quad (5)$$

(17) Ooi, B.-L.; Sykes, A. G. *Inorg. Chem.* **1989**, *28*, 3799.
(18) Tobias, R. S. *Acta Chem. Scand.* **1958**, *12*, 198.
(19) Johnson, J. S.; Kraus, K. A. *J. Phys. Chem.* **1959**, *63*, 440.
(20) Vogel, A. L. In *Textbook of Macro and Semimicro Quantitative Inorganic Analysis*, 5th ed.; revised by Svehla, G.; Longman: London, 1979; pp 237−241. Both Sn^{II} and Sn^{IV} give a white precipitate on addition of NaOH (excess to be avoided).

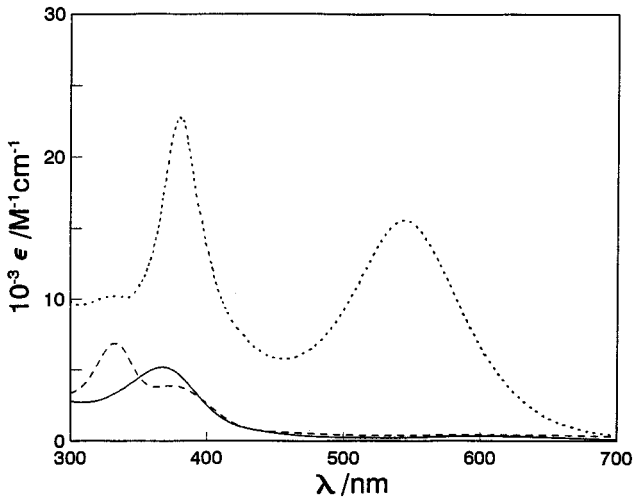

Figure 2. UV−vis spectra of $Mo_6SnS_8^{8+}$, ϵ's per Mo_6 (···), $Mo_3SnS_4^{6+}$, ϵ's per Mo_3 (- - -), and $Mo_3S_4^{4+}$, ϵ's per Mo_3 (—), in 2.0 M Hpts.

Table 2. Crystallographic Data

formula	$C_{21}H_{49}Cl_3Mo_3N_{15}O_{0.5}S_{13}Sn$	fw	1449.4
a/Å	42.258(14)	space group	$C2/c$
b/Å	11.907(3)	temp/K	160
c/Å	21.472(5)	λ/Å	0.710 73
β/deg	94.449(9)	D(calc)/g cm^{-3}	1.788
V/Å^3	10771(5)	μ/mm^{-1}	1.83
R^a	0.0817	Z	8
$R_w{}^a$	0.1563		

[a] Conventional $R = \sum||F_o| - |F_c||/\sum|F_o|$ for reflections with $F_o^2 > 2\sigma(F_o^2)$; $R_w = [\sum[w(F_o^2 - F_c^2)^2]/\sum[w(F_o^2)^2]]^{1/2}$ for all data.

However there is a possibility that Sn^{IV} build-up will occur under these conditions as O_2 accesses the solution.

Other Reagents. Solid $NH_4[Co(dipic)_2]$ (dipic = 2,6-dicarboxylatopyridine), peak at 510 nm (ϵ = 630 M^{-1} cm^{-1}), was prepared as previously.[21] Solutions of $[Fe(H_2O)_6]^{3+}$ were obtained from iron(III) perchlorate (Fluka) and purified by loading on a Dowex 50W-X2 column. Elution was with 0.50−1.00 M Hpts. The concentration of Fe^{III} was determined by reduction with hydroxylamine hydrochloride (Aldrich) and determining the Fe^{II} formed after complexing with 1,10-phenanthroline to give $[Fe(phen)_3]^{2+}$, peak at 510 nm ($\epsilon = 10.9 \times 10^3$ M^{-1} cm^{-1}).

Crystallographic Studies for $[Me_2NH_2]_6$ $[Mo_3S_4SnCl_3(NCS)_9]\cdot 0.5H_2O$. A crystal of dimensions 0.28 × 0.24 × 0.08 mm was examined on a Siemens SMART CCD diffractometer with graphite-monochromated Mo Kα radiation. Crystal data are listed in Table 2. The cell parameters were refined from the setting angles and recorded spot positions of 170 reflections (θ = 1−24°) measured on a series of oscillation frames. Intensities were integrated from more than a hemisphere of data recorded on 0.3° frames by ω rotation over a total time of 10 h. Semiempirical absorption corrections were applied on the basis of equivalent data (transmission 0.692−0.819). A total of 21 116 measured reflections yielded 7728 unique data (R_{int} = 0.0609), 7193 of which were "observed" with $F_o^2 > 2\sigma(F_o^2)$.

The structure was determined by direct methods and refined by full-matrix least-squares procedures on F^2 for all data, with weighting $w^{-1} = \sigma^2(F_o^2) + 301.4P$, where $P = (F_o^2 + 2F_c^2)/3$. Anisotropic displacement parameters were refined for all non-H atoms, and isotropic H atoms were included with riding model constraints. Disorder was resolved and refined for one of the cations, with the aid of similarity restraints on geometry and displacement parameters, and for the water molecule, which is disordered over two sites close to a rotation axis. A total of 542 parameters were refined. All shift/esd ratios in the final cycle were <0.01, and difference map features were in the range +1.05 to −0.74 e Å^{-3}, the largest peaks being close to the disordered cation. Programs were standard Siemens control (SMART) and integration (SAINT) software, SHELXTL,[22] and local programs. Atomic coordinates for the anion are listed in Table 3, with selected bond lengths and angles in Table 4.

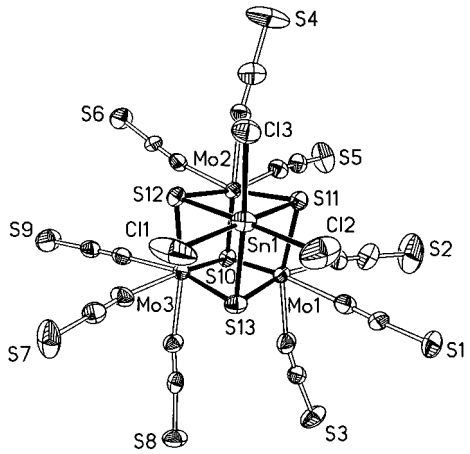

Figure 3. View of the anion of the single cube $[Mo_3(SnCl_3)S_4(NCS)_9]^{5-}$ with 50% probability ellipsoids and atomic labeling. Thiocyanate N and C atoms are numbered as the corresponding S atoms.

Table 3. Atomic Coordinates (×10^4) and Equivalent Isotropic Displacement Parameters (Å^2 × 10^3) for the Anion

	x	y	z	U
Mo1	3601.7(2)	4818.3(8)	5535.9(5)	22.8(2)
Mo2	3761.2(2)	2987.8(8)	4867.7(4)	21.6(2)
Mo3	4137.6(2)	3619.7(8)	5898.5(4)	22.5(2)
S10	4054.9(6)	4654(2)	4968.9(13)	24.2(6)
S11	3271.1(7)	3275(2)	5284.0(13)	26.7(7)
S12	3909.2(7)	1838(2)	5728.7(14)	26.9(7)
S13	3730.6(7)	4081(3)	6526.7(13)	29.4(7)
Sn1	3404.0(2)	2222.7(7)	6367.8(4)	32.2(2)
C11	3650.0(13)	1394(4)	7338(2)	81(2)
C12	2936.9(11)	2887(4)	6864(2)	84(2)
C13	3140.0(8)	414(3)	6097(2)	44.3(8)
N1	3197(2)	5492(9)	5968(5)	33(2)
C1	2985(3)	5808(11)	6228(6)	33(3)
S1	2669.7(8)	6295(4)	6556(2)	55.8(11)
N2	3374(2)	5731(9)	4761(5)	32(2)
C2	3246(3)	6307(13)	4397(7)	49(4)
S2	3061.2(14)	7145(5)	3892(3)	97(2)
N3	3785(2)	6466(10)	5770(5)	36(3)
C3	3841(3)	7424(11)	5804(5)	30(3)
S3	3907.5(9)	8777(3)	5817(2)	46.2(9)
N4	3527(2)	1525(9)	4428(5)	31(2)
C4	3398(3)	984(12)	4039(6)	40(3)
S4	3220.0(12)	228(5)	3481(2)	81(2)
N5	3606(2)	3686(9)	3978(5)	30(2)
C5	3564(3)	4174(11)	3507(6)	31(3)
S5	3514.7(9)	4882(4)	2864(2)	54.4(11)
N6	4151(2)	2339(8)	4366(5)	31(2)
C6	4332(3)	1953(10)	4051(6)	29(3)
S6	4583.8(8)	1437(3)	3593(2)	46.6(9)
N7	4352(2)	2880(9)	6747(5)	34(2)
C7	4433(3)	2538(11)	7227(6)	36(3)
S7	4564.0(10)	2059(4)	7929(2)	67.8(14)
N8	4392(2)	5075(9)	6264(5)	30(2)
C8	4480(3)	5904(11)	6496(5)	28(3)
S8	4622.4(8)	7028(3)	6855(2)	41.3(8)
N9	4583(2)	3167(8)	5559(4)	31(2)
C9	4829(3)	2936(10)	5382(6)	33(3)
S9	5172.6(8)	2650(4)	5132(2)	64.5(13)

Kinetic Studies. These were carried out at 25.0 ± 0.1 °C and ionic strength I = 2.00 ± 0.02 M adjusted with Li(pts). Absorbance changes were monitored on a Dionex D-110 stopped-flow spectrophotometer. Standard air-free (N_2) techniques were used throughout. The spectrophotometer was interfaced to an IBM PC/AT-X computer for data acquisition using software from On-Line Instrument Systems (Bogart,

(21) Mauk, A. G.; Coyle, C. L.; Bordignon, E.; Gray, H. B. *J. Am. Chem. Soc.* **1979**, *101*, 5054.

(22) Sheldrick, G. M. *SHELXTL User Manual*; Siemens Analytical X-ray Instruments Inc.: Madison, WI, 1994.

Table 4. Selected Bond Lengths (Å) and Bond Angles (deg)

Mo1−S10	2.356(3)	Mo1−S11	2.346(3)
Mo1−S13	2.327(3)	Mo2−S10	2.342(3)
Mo2−S11	2.343(3)	Mo2−S12	2.346(3)
Mo3−S10	2.348(3)	Mo3−S12	2.347(3)
Mo3−S13	2.332(3)	Mo1−N1	2.162(10)
Mo1−N2	2.152(11)	Mo1−N3	2.154(12)
Mo2−N4	2.182(10)	Mo2−N5	2.139(10)
Mo2−N6	2.178(10)	Mo3−N7	2.158(10)
Mo3−N8	2.155(10)	Mo3−N9	2.138(10)
S11−Sn1	2.664(3)	S12−Sn1	2.666(3)
S13−Sn1	2.616(3)	Sn1−C11	2.461(4)
Sn1−C12	2.446(4)	Sn1−C13	2.474(3)
Mo1−Mo2	2.723(2)	Mo1−Mo3	2.738(2)
Mo2−Mo3	2.729(2)		

S13−Mo1−S11	90.46(11)	S13−Mo1−S10	107.42(11)
S11−Mo1−S10	108.02(11)	S10−Mo2−S11	108.59(11)
S10−Mo2−S12	108.32(11)	S11−Mo2−S12	88.52(11)
S13−Mo3−S12	89.42(11)	S13−Mo3−S10	107.48(11)
S12−Mo3−S10	108.04(11)	Mo2−S10−Mo3	71.17(9)
Mo2−S10−Mo1	70.85(8)	Mo3−S10−Mo1	71.19(8)
Mo2−S11−Mo1	70.98(9)	Mo2−S11−Sn1	97.58(10)
Mo1−S11−Sn1	94.91(10)	Mo2−S12−Mo3	71.11(9)
Mo2−S12−Sn1	97.47(10)	Mo3−S12−Sn1	95.78(10)
Mo1−S13−Mo3	71.98(9)	Mo1−S13−Sn1	96.68(11)
Mo3−S13−Sn1	97.52(11)	S13−Sn1−S11	77.85(9)
S13−Sn1−S12	77.11(9)	S11−Sn1−S12	75.77(9)

GA). All quoted rate constants are the average of at least five determinations using the same solutions.

Results

Crystallographic Studies. The structure of the anion $[Mo_3(SnCl_3)S_4(NCS)_9]^{6-}$ is shown in Figure 3. Features to note are the bond lengths Mo−S 2.327(3)−2.356(3) Å (mean 2.343 Å) and Mo−N 2.138(10)−2.182(10) Å (mean 2.158 Å). Angles at the N atoms vary widely, 158.3(10)−178.6(9)°, and appear to be easily affected by crystal packing forces. The N−C−S is close to linear in all cases with angles ≥176.0°. Other bond lengths are Sn−S 2.616(3)−2.666(3) Å and Sn−Cl 2.446(4)−2.474(3) Å. The distances Mo−Mo 2.723−2.738 (mean 2.730 Å) and Mo−Sn 3.698−3.773 (mean 3.732 Å) indicate an Mo−Mo and Mo−Sn difference of 1 Å.

Stoichiometries for Oxidations of $[Mo_3SnS_4(H_2O)_{12}]^{6+}$. The oxidations of $[Mo_3SnS_4(H_2O)_{12}]^{6+}$ in 2.0 M Hpts were determined by monitoring absorbance changes on addition of aliquots of (i) $[Co(dipic)_2]^-$ and (ii) $[Fe(H_2O)_6]^{3+}$ until no further changes occurred. The time scale of the experiments was ∼1 h at 25 °C. During this time, control experiments indicated <1% $[Co(dipic)_2]^-$ oxidation of free Sn^{II}, in agreement with previous studies of Sn^{II} reductions of Co^{III} complexes,[23] and negligible $[Fe(H_2O)_6]^{3+}$ oxidation of Sn^{II} is observed.[23,24] Stoichiometries (±3%) expressed as oxidant:$Mo_3SnS_4^{6+}$ of 2.15:1 (Co) and 2.05:1 (Fe) were determined, consistent with (6) and (7). A mechanism involving decomposition of $Mo_3SnS_4^{6+}$ and/or $Mo_3SnS_4^{8+}$ (both transients) is indicated.

$$Mo_3SnS_4^{6+} + 2Co^{III} \rightarrow Mo_3S_4^{4+} + Sn^{IV} + 2Co^{II} \quad (6)$$

$$Mo_3SnS_4^{6+} + 2Fe^{III} \rightarrow Mo_3S_4^{4+} + Sn^{IV} + 2Fe^{II} \quad (7)$$

Stoichiometries for Oxidations of $[Mo_6SnS_8(H_2O)_{18}]^{8+}$. From the absorbance decay of the $[Mo_6SnS_8(H_2O)_{18}]^{8+}$ double cube at 540 nm, the stoichiometry of the $[Co(dipic)_2]^-$ oxidation was determined as 3.6:1 (in 2.0 M Hpts) and 4.0:1 (in 2.0 M HCl). The product is $[Mo_3S_4(H_2O)_9]^{4+}$ (see eq 8). It was possible to monitor the corresponding $[Fe(H_2O)_6]^{3+}$ oxidation at 540 nm (decay of $Mo_6SnS_8^{8+}$) and 330 nm, when evidence for intermediate formation of $Mo_3SnS_4^{6+}$ (Figure 1) was obtained, Figure 4. The overall stoichiometry determined at 540 nm was 3.72:1 and the final product was $[Mo_3S_4(H_2O)_9]^{4+}$, consistent with (9), as the dominant process.

$$Mo_6SnS_8^{8+} + 4Co^{III} \rightarrow 2Mo_3S_4^{4+} + Sn^{IV} + 4Co^{II} \quad (8)$$

$$Mo_6SnS_8^{8+} + 4Fe^{III} \rightarrow 2Mo_3S_4^{4+} + Sn^{IV} + 4Fe^{II} \quad (9)$$

Interconversion of Single and Double Cubes. The conversion of $[Mo_6SnS_8(H_2O)_{18}]^{8+}$ to $[Mo_3SnS_4(H_2O)_{10}]^{6+}$ by adding a 2:1 excess of either Co^{III} or Fe^{III} oxidant (as above) was carried out with up to 70% recovery of the single cube using cation-exchange chromatography. Conversely, the reverse was achieved by mixing 1:1 amounts of $[Mo_3SnS_4(H_2O)_{12}]^{6+}$ and $[Mo_3S_4(H_2O)_9]^{4+}$ in 1.0 M Hpts and using a 100-fold excess of BH_4^- as reductant. Column chromatography gives ∼50% yields of the double cube $[Mo_6SnS_8(H_2O)_{18}]^{8+}$.[25]

Reaction of Sn Cubes with Cl^-. The single cube $[Mo_3SnS_4(H_2O)_{12}]^{6+}$ in 2.0 M Hpts shows a high affinity for Cl^- monitored at 384 nm, with complete complexation observed at $[Cl^-] \geq 0.050$ M, Figure 5. On loading $Mo_3SnS_4^{6+}$ and $Mo_3S_4^{4+}$ onto a Dowex 50W-X2 cation-exchange column and eluting with 1.0 M HCl, $Mo_3SnS_4^{6+}$ elutes first (as compared to second with Hpts or $HClO_4$). The implication is that the charge on $Mo_3SnS_4^{6+}$ is <4 and that three Cl^-'s are coordinated to the Sn as in (10). The involvement of three chlorides is

$$Mo_3SnS_4^{6+} + 3Cl^- \rightarrow Mo_3(SnCl_3)S_4^{3+} \quad (10)$$

supported by the crystal structure of $[Mo_3(SnCl_3)S_4(NCS)_9]^{6-}$. Assuming >90% product formation in (10) with $[Cl^-] = 0.05$ M, $K > 10^2$ M^{-3}. The 1:1 complexing of Cl^- to $[Mo_4S_4(H_2O)_{12}]^{5+}$ ($K = 1.98$ M^{-1})[26] and to $[Mo_3S_4(H_2O)_9]^{4+}$ ($K = 3.0$ M^{-1})[27] is much less extensive, $I = 2.00$ M ($LiClO_4$).

In the case of the double cube $[Mo_6SnS_8(H_2O)_{18}]^{8+}$ in 2.0 M Hpts (or $HClO_4$), addition of $[Cl^-] \geq 0.50$ M gives absorbance changes corresponding to the formation of $[Mo_3(SnCl_3)S_4(H_2O)_9]^{3+}$ and $[Mo_3S_4(H_2O)_9]^{4+}$. Using this approach with $[Cl^-] = 1.25$ M, $[H^+] = 2.0$ M, and $I = 2.0$ M (ClO_4^-), the reaction is ∼40% complete in ∼1 h. The high affinity of Cl^- for the central Sn atom results in the cleavage of the double cube with formation of e.g. $Mo_3S_4^{2+}$ as a transient, (11). The absorbance changes indicate that other products may be involved.

$$Mo_6SnS_8^{8+} + 3Cl^- \rightarrow Mo_3(SnCl_3)S_4^{3+} + Mo_3S_4^{2+} \quad (11)$$

Kinetic Studies on the Oxidation of $[Mo_6SnS_8(H_2O)_{18}]^{8+}$. Observations illustrated in Figure 4 indicate a sequence $Mo_6SnS_8^{8+} \rightarrow Mo_3SnS_4^{6+} + Mo_3S_4^{4+} \rightarrow 2\ Mo_3S_4^{4+} + Sn^{IV}$ for the Fe^{III} (or Co^{III}) oxidation of the double cube $[Mo_6SnS_8(H_2O)_{18}]^{8+}$. Larger absorbance changes were obtained for the double to single cube conversion, as compared with changes for oxidation of the single cube to $[Mo_3S_4(H_2O)_9]^{4+}$. Kinetic studies correspond to the $Mo_6SnS_8^{8+} \rightarrow Mo_3SnS_4^{6+}$ change.

Uniphasic kinetics are observed for both the $[Co(dipic)_2]^-$ and $[Fe(H_2O)_6]^{3+}$ oxidations of $Mo_6SnS_8^{8+}$ monitored at 580 and 540 nm, respectively, and the kinetics indicate a reaction

(23) Wetton, E. A. M.; Higginson, W. C. E. *J. Chem. Soc.* **1965**, 5890.
(24) Gorin, M. H. *J. Am. Chem. Soc.* **1936**, *58*, 1787.
(25) Saysell, D. M.; Sokolov, M. N.; Sykes, A. G. *Sulfur Coordinated Transition Metal Complexes*; ACS Symposium Series; American Chemical Society: Washington, DC, in press.
(26) Li, Y.-J.; Nasreldin, M.; Humanes, M.; Sykes, A. G. *Inorg. Chem.* **1992**, *31*, 3011.
(27) Richens, D. T.; Pittet, P.-A.; Merbach, A. E.; Humanes, M.; Lamprecht, G. J.; Ooi,, B.-L.; Sykes, A. G. *J. Chem. Soc., Dalton Trans.* **1993**, 2305.

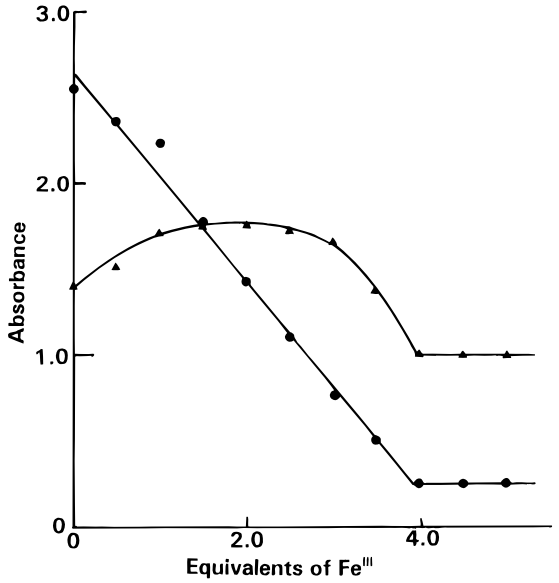

Figure 4. Stoichiometry determination for the reaction of $[Fe(H_2O)_6]^{3+}$ with $Mo_6SnS_8^{8+}$. Titration of aliquots (0.005 mL) of Fe^{III} (6.1×10^{-5} M) to $Mo_6SnS_8^{8+}$ (2.5 mL of 1.23×10^{-4} M) was monitored at 540 nm (●) and 330 nm (▲).

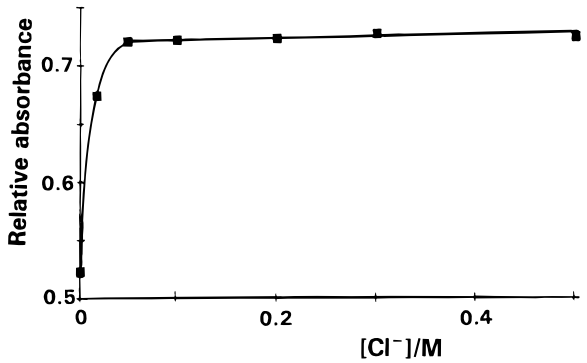

Figure 5. Increase in absorbance at 384 nm upon addition of Cl^- to $Mo_3SnS_4^{6+}$ in $HClO_4$. $[H^+] = 2.00$ M; $[ClO_4^-] + [Cl^-] = 2.00$ M.

Table 5. First-Order Rate Constants k_{obs} (25 °C) for the Oxidation of $[SnMo_6S_8(H_2O)_{18}]^{8+}$ ($\sim 3.3 \times 10^{-5}$ M) with $[Co(dipic)_2]^-$, at Different $[H^+]$ and $[Co(dipic)_2^-]$ Values, $\lambda = 580$ nm, $I = 2.00$ M (Li(pts))

$[H^+]$/M	10^3[Co(III)]/M	10^2k_{obs}/s^{-1}	$[H^+]$/M	10^3[Co(III)]/M	10^2k_{obs}/s^{-1}
2.00	1.0	1.50	1.00	1.0	1.49
	2.0	3.0		2.0	2.73
	3.0	4.6		3.0	4.7
	4.0	6.1		4.0	5.6
1.50	1.0	1.41	0.50	2.0	2.97
	3.0	4.5		4.0	6.0
	5.0	7.4		7.0	10.4
	7.0	10.4		9.2	13.8
				13.3	19.7 (19.6)[a]

[a] $\lambda = 600$ nm.

sequence involving $Mo_6SnS_8^{9+}$ as a transient. Fragmentation of the double cube structure must also occur. First-order rate constants k_{obs}, Table 5, define the rate law (12), and $k_{Co} = 14.9$

$$-d[Mo_6SnS_8^{8+}]/dt = k_{Co}[Mo_6SnS_8^{8+}][Co(dipic)_2^-] \quad (12)$$

± 0.1 M^{-1} s^{-1}, which is independent of $[H^+] = 0.50-1.90$ M. The corresponding data for Fe^{III}, Table 6, define k_{Fe} values, Table 6. The linear $[H^+]^{-1}$ dependence, Figure 6, is summarized

Table 6. First-Order Rate Constants k_{obs} (25 °C) for the Oxidation of $[SnMo_6S_8(H_2O)_{18}]^{8+}$ ($\sim 3.3 \times 10^{-5}$ M) with $[Fe(H_2O)_6]^{3+}$, at Different $[H^+]$ and $[Fe^{III}]$ Values, $\lambda = 540$ nm, $I = 2.00$ M (Li(pts))[a]

$[H^+]$/M	10^3[Fe(III)]/M	10^2k_{obs}/s^{-1}	$[H^+]$/M	10^3[Fe(III)]/M	10^2k_{obs}/s^{-1}
1.90[b]	1.0	0.42	0.75[e]	1.0	1.00
	3.0	1.24		3.0	3.01
	4.0	1.66		5.0	5.0
	6.0	2.49		7.0	7.1
	8.7	3.6		8.7	8.8
1.50[c]	3.0	1.55	0.50[f]	2.0	2.90
	4.0	2.06		3.0	4.3
	5.0	2.58		5.0	7.2
	6.0	3.10		7.0	10.0
	8.7	4.5		8.7	12.4
1.00[d]	3.0	2.30			
	4.0	3.05			
	5.0	3.8			
	6.0	4.5			
	8.7	6.6			

[a] The data are plotted in Figure 7, and second-order rate constants k_{Fe} from the slopes are as indicated in the following footnotes. [b] 4.2. [c] 5.2. [d] 7.6. [e] 10.2. [f] 14.2.

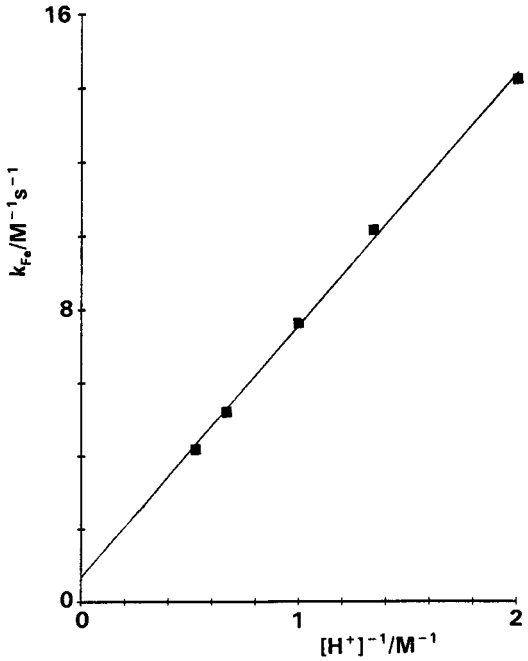

Figure 6. Variation of second-order rate constants k_{Fe} (25 °C) with $[H^+]^{-1}$ for the $[Fe(H_2O)_6]^{3+}$ oxidation of $Mo_6SnS_8^{8+}$, $I = 2.00$ M (Li(pts)).

by (13), with $k_a = 0.68 \pm 0.23$ M^{-1} s^{-1} and $k_b = 6.9 \pm 0.2$

$$k_{Fe} = k_a + k_b[H^+]^{-1} \quad (13)$$

s^{-1}. These two terms are assigned to the reaction of $[Fe(H_2O)_6]^{3+}$ ($pK_a = 3.0$ at 25 °C, $I = 2.0$ M ($NaClO_4$)[28]) and $[Fe(H_2O)_5(OH)]^{2+}$, respectively.

Reactions with Cu^{II}. The double cube $[Mo_6SnS_8(H_2O)_{18}]^{8+}$ (0.36 mM) in 2.0 M Hpts reacts with Cu^{II} (7.0 mM) to give the red-brown product $[Mo_3CuS_4(H_2O)_{10}]^{5+}$ which has a UV−vis spectrum with peaks λ/nm (ϵ/M^{-1} cm^{-1} per cube) at 328 (5130)and 472 (2200) and no peak at 975 nm. The cube $[Mo_3CuS_4(H_2O)_{10}]^{4+}$ has a markedly smaller absorbance at 325 (3700) and a peak at 975 nm as compared to the 5+ form. No similar reaction is observed with $[Mo_3SnS_4(H_2O)_{12}]^{6+}$ also in 2.0 M Hpts.

(28) Baes, C. F.; Mesmer, R. E. *Hydrolysis of Cations*; Wiley: New York, 1976; p 230.

Discussion

An X-ray crystal structure of the single cube $Mo_3SnS_4^{6+}$, Figure 3, firmly establishes this form alongside the double cube $Mo_6SnS_8^{8+}$ reported previously.[9] The cluster present as $[Mo_3(SnCl_3)S_4(NCS)_9]^{6-}$ is isostructural with the corresponding W_3 compound,[29] with Mo−Mo (2.730 Å) virtually identical to W−W (2.735 Å). Similarly, the core Mo−S and W−S distances are identical (2.343 Å). Long Mo−Sn (3.732 Å) and W−Sn (3.817 Å) distances indicate little or no metal−metal bonding to the Sn. However the Sn−S bonds are shorter by 0.092 Å in the Mo cluster, implying that $SnCl_3$ is more strongly bonded. This suggests more Sn^{II} character in the W_3 cube, consistent with the greater difficulty in reducing W.[30] Comparisons of Sn−Cl (2.460 Å) with those in $(NH_4)_2[SnCl_3]Cl\cdot H_2O$ (2.50 Å) and $[SnCl_6]^{2-}$ (2.42 Å) are also of interest.[31,32]

The demonstration that the Mo_3SnS_4 core has a 6+ charge confirms an earlier proposal of Shibahara and colleagues.[9] The preparation of $[Mo_3SnS_4(H_2O)_{12}]^{6+}$ is unusual in that it involves direct addition of Sn^{2+} to $[Mo_3S_4(H_2O)_9]^{4+}$ in a rapid process. The only previous example of this type of reaction is the addition of Cu^+ to $[Mo_3S_4(H_2O)_9]^{4+}$ giving $[Mo_3CuS_4(H_2O)_{10}]^{5+}$.[14] Formation of $Mo_6SnS_8^{8+}$ by the reaction $[Mo_3S_4(H_2O)_9]^{4+}$ with the metal is a more widely observed process.

The high affinity of the Sn of $Mo_3SnS_4^{6+}$ for Cl^- allows separate complexing of Sn (by Cl^-) prior to Mo (by NCS^-) in preparing crystalline samples. The affinity of Sn for Cl^- is confirmed by the completion of absorbance changes for 0.13 mM cube with as little as 0.05 M Cl^-, Figure 5. From cation-exchange behavior, using 1.0 M HCl, elution occurs prior to $Mo_3S_4^{4+}$, and binding of three Cl^- ions is indicated. In contrast, Mo displays little affinity for Cl^-.[26,27] In keeping with the six-coordination which the Sn displays in the presence of Cl^-, we assume a formula for the aqua ion $[Mo_3SnS_4(H_2O)_{12}]^{6+}$ in 2.0 M $HClO_4$ and 2.0 M Hpts. Addition of Cl^- (1.25 M) to $Mo_6SnS_8^{8+}$ is a somewhat different process in that it induces a redox change with fragmentation to give $Mo_3(SnCl_3)S_4^{3+}$ and $Mo_3S_4^{4+}$. The reaction is unexpected in that Mo in such clusters is normally inert to substitution, and the Cl^- therefore very likely accesses the Sn already bonded to six core sulfides. Since there is no obvious oxidant, the involvement of H^+ and/or ClO_4^- is possible. The reaction suggests that Cl^- has a stronger affinity for $Mo_3SnS_4^{6+}$ than Mo_3S_4, which it displaces.

As far as the properties of heterometallic cubes are concerned, the reluctance to undergo redox change with retention of the cube structure is in contrast to the behavior of $[Mo_4S_4(H_2O)_{12}]^{n+}$, which gives clusters of charge $n = 4-6$.[33] So far, only $[Mo_3CuS_4(H_2O)_{10}]^{n+}$ ($n = 4$, 5) behave in a similar manner.[14] Oxidation normally results in release of the heterometal atom with the formation of $[Mo_3S_4(H_2O)_9]^{4+}$.[34] The redox-induced interconversion of single and double cubes is one of the main results of the present study. It is observed that the first $2e^-$ oxidation of $Mo_6SnS_8^{8+}$ yields $Mo_3SnS_4^{6+}$ (up to 70% recovery) with release of $Mo_3S_4^{4+}$. The $Mo_3SnS_4^{6+}$ is then further $2e^-$ reduced with the formation of $Mo_3S_4^{4+}$ and Sn^{IV}, (14).

$$Mo_6SnS_8^{8+} - 4e^- \rightarrow 2Mo_3S_4^{4+} + Sn^{IV} \qquad (14)$$

Conversely BH_4^- reduction of a 1:1 mixture of $[Mo_3SnS_4(H_2O)_{10}]^{6+}$ and $[Mo_3S_4(H_2O)_9]^{4+}$ gives $[Mo_6SnS_8(H_2O)_{18}]^{8+}$ with ∼50% yield after column chromatography.[25] The reverse reaction involving addition of Sn^{IV} to $[Mo_3S_4(H_2O)_9]^{4+}$ is not observed. The 6+ and 8+ charges on the single and double cubes, respectively, are confirmed by redox stoichiometry measurements combined with product determination.

Kinetic studies on the reactions of the double cube $Mo_3SnS_4^{8+}$ with $[Co(dipic)_2]^-$ and $[Fe(H_2O)_6]^{3+}$ as oxidants give rate laws first-order in each reactant, with transient $Mo_6SnS_8^{9+}$ involvement implied. The reactions of $[Co(dipic)_2]$ (k_{Co}) and $[Fe(H_2O)_6]^{3+}$ (k_a), but not $[Fe(H_2O)_5OH]^{2+}$ (k_b), are assigned as outer-sphere electron-transfer processes. The log values of $k_{Co} = 14.9\ M^{-1}\ s^{-1}$ and $k_a = 0.68\ M^{-1}\ s^{-1}$ give good agreement with the linear correlation previously observed for a number of heterometallic cubes.[34] This is however the first entry for a corner-shared double cube.

While it is tempting to view the $2e^-$ redox interconversion of $Mo_6SnS_8^{8+}$ and $Mo_3SnS_4^{4+}$ in terms of Sn^{II} and Sn^{IV} participation, such assignments are not always clearcut.[13b] Here it might be argued that Sn^{II} is a component of the double cube and that $Mo_6SnS_8^{8+}$ is $2e^-$ oxidized to the single cube $Mo_3SnS_4^{6+}$. It therefore follows that Sn^{IV} is present in $Mo_3SnS_4^{6+}$ (and has high affinity for Cl^-), with the Mo_3 unit present as $Mo^{III}_2Mo^{IV}$. If this is the case, then charge transfer occurs on formation of the double cube (from Sn) and the single cube (from Sn^{II}).

Finally the reaction of Cu^{II} with $Mo_6SnS_8^{8+}$ yielding $Mo_3CuS_4^{5+}$ is similar to the reactions of Cu^{II} with e.g. $Mo_3FeS_4^{4+}$ and $Mo_3NiS_4^{4+}$.[35] As previously, a mechanism involving electron transfer is suggested with intermediate formation of Cu^I and $Mo_3S_4^{4+}$.[14] Although Cu^{II} is not a strong oxidant, the setting up of an equilibrium such as (15) leads to rapid formation

$$Mo_6SnS_8^{8+} + 2Cu^{II} \rightleftarrows Mo_3SnS_4^{6+} + Mo_3S_4^{4+} + 2Cu^I \qquad (15)$$

of the product, (16), in an additional step. No corresponding

$$Mo_3S_4^{4+} + Cu^I \rightarrow Mo_3CuS_4^{5+} \qquad (16)$$

reaction of $Mo_3SnS_4^{6+}$ is observed, which suggests that $Mo_6SnS_8^{8+}$ is more readily oxidized by Cu^{II} than $Mo_3SnS_4^{6+}$.

Acknowledgment. We are grateful to the U.K. Science and Engineering Research Council (now EPSRC) for a studentship and the SCI for a Messel Scholarship (both to J.E.V.), to the University of the Orange Free State in Bloemfontein for a leave of absence and the EPSRC for support (to G.J.L.), to the Leverhulme Trust and the University of Barbados in the West Indies for financial support and a study leave (to A.H.), and to the Royal Society for a Kapitza Fellowship (to V.P.F.). W.C. has also received generous support from the EPSRC.

Supporting Information Available: One X-ray crystallographic file, in CIF format, is available. Access information is given on any current masthead page.

IC951659M

(29) Müller, A.; Fedin, V. P.; Diemann, E.; Bögge, H.; Krickemeyer, E.; Sölter, D.; Giuliana, A. M.; Barbieri, R.; Adler, P. *Inorg. Chem.* **1994**, *33*, 2243.
(30) Ooi, B.-L.; Petrou, A. L.; Sykes, A. G. *Inorg. Chem.* **1988**, *27*, 3626.
(31) Harrison, P. G.; Haylett, B. J.; King, T. J. *Inorg. Chim. Acta* **1983**, *75*, 265.
(32) Jaulmes, S.; Julien-Pouzol, M.; Laruelle, P.; Guittard, M. *Acta Crystallogr.* **1982**, *B38*, 79.
(33) Ooi, B.-L.; Sharp, C.; Sykes, A. G. *J. Am. Chem. Soc.* **1989**, *111*, 125.
(34) Dimmock, P. W.; Saysell, D. M.; Sykes, A. G. *Inorg. Chim. Acta* **1994**, *225*, 157.
(35) Shibahara, T.; Asano, T.; Sakane, G. *Polyhedron* **1991**, *10*, 2351.